# Electrochemical Properties of Permeable Multichain Polyamino Acids

**Harold A. Scheraga,[1] Aharon Katchalsky, and Zipora Alterman**

*Contribution from the Department of Chemistry, Cornell University, Ithaca, New York 14850, and the Weizmann Institute of Science, Rehovoth, Israel.*
*Received February 12, 1969*

**Abstract:** Several electrochemical properties (the titration curve, Donnan distribution of counterions, and osmotic properties) of permeable multichain polyelectrolyte molecules at *finite* polymer concentration, in the presence and absence of salt, have been computed. The model used for the calculation of the electrostatic potential, $\psi$, is a permeable cylinder with a uniform distribution of the *fixed* charges. The Poisson–Boltzmann equation was solved numerically, with the boundary conditions that the potential and gradient of the potential, respectively, are equal on both sides of the surface of the macromolecule. The dimensions of the cylinder correspond to those for a multichain polymer in which the polyamino acid chains are either in the $\alpha$-helical or fully stretched conformations, respectively. The model is thus applicable for evaluation of the electrochemical properties of multichain polyamino acids in which a helix → fully stretched transformation may occur as the degree of ionization of the charged groups increases. The computed titration curves are in agreement with those obtained by Goldstein[2] for a multichain poly-L-glutamic acid, taking cognizance of the effect of conformation on $pK_0$. The theory may also be applicable to proteins and nucleic acids.

Goldstein[2] has examined the titration curves of some multichain polyamino acids.[3,4] The multichain polymers are prepared, for example, by using the $\epsilon$-amino groups of a poly-L-lysine chain to initiate the polymerization of $\gamma$-benzyl-N-carboxyl-L-glutamate anhydride; debenzylation yields the corresponding multichain polyglutamic acid.

Since the multichain polyamino acids have a cross section into which small ions may penetrate, these polymers are useful models for the study of the electrochemical and transport properties of charged branched macromolecules. The aim of this paper is to develop a theory to account for some of the electrochemical properties of such macromolecules, *viz.*, the titration curve, Donnan distribution of counter ions, and osmotic properties. While the theory will be applied here to Goldstein's data[2] on the multichain polymer, it may have applicability to other macromolecules, such as globular proteins and nucleic acids, which are also penetrable by small ions. From one point of view, the multichain polymer may also serve as a model for a charged biological membrane, through which ions may pass.

The multichain polymer, being an ionizable macromolecule, consists of a discrete number of inner charges, and will give rise to an unequal distribution of the counterions and co-ions inside and outside the molecule. Our primary interest is in the computation of the equilibrium properties of such a system. These, in turn, are derivable from the electrostatic potential[5] which will be computed here.

## The Model

A schematic model of a multichain polymer will be used as a basis for the calculation of the electrostatic potential $\psi$. A polymer consisting of a polylysine backbone and polyglutamic acid branches may be regarded as having the shape of a prolate ellipsoid of revolution. Since the major contribution to the local potential, at finite salt concentration, is made by the ionic species in the immediate neighborhood of any charge, end effects may be neglected as an approximation. In the presence of salt, the ellipsoid can therefore be approximated by a cylinder, which is much simpler to treat mathematically. The cylindrical approximation becomes better for larger backbones (compared to the branches) and for increasing ionic strength. The cylinder is considered to have a length $h$ and radius $a$ (see Figure 1). The values of $h$ and $a$ will depend on the conformations of the various chains of the molecule; as illustrative cases, we have chosen extreme values of these parameters which correspond to $\alpha$-helical and fully stretched conformations, respectively. Therefore, the computed electrochemical properties will not only be those of the two conformations mentioned, but will also be useful for a consideration of the transformation between the $\alpha$-helical and fully stretched conformations.

Since it is possible to titrate all the carboxyl groups,[2] the molecule must be permeable to the solvent. However, we cannot utilize previous theories of permeable molecules[6] since they are based on the Debye–Hückel approximation, *i.e.*, that $\epsilon\psi/kT << 1$, a condition which does not hold for multichain polyamino acids even at moderate degrees of ionization. Since the Poisson–Boltzmann equation (without the Debye–Hückel linearization of the exponential) is regarded as a reasonable approximation for the study of polyelectrolyte solutions,[7] we will treat the permeable cylinder by solving

(1) This work was begun in 1963 while H. A. S. was a Fulbright Research Scholar and Guggenheim Fellow at the Weizmann Institute. Subsequent support, at Cornell University, was received from a research grant (GB-7571X) from the National Science Foundation, and from a research grant (GM-14312) from the National Institute of General Medical Sciences of the National Institutes of Health, U. S. Public Health Service.

(2) L. Goldstein, Ph.D. Thesis, Hebrew University, Jerusalem, March 1963.

(3) E. Katchalski, M. Sela, H. I. Silman, and A. Berger in "The Proteins," Vol. II, 2nd ed, H. Neurath, Ed., Academic Press, New York, N. Y., 1964, p 405.

(4) A. Berger and A. Yaron in "Polyamino Acids, Polypeptides, and Proteins," M. A. Stahmann, Ed., University of Wisconsin Press, Madison, Wis., 1962, p 13.

(5) A. Katchalsky, Z. Alexandrowicz, and O. Kedem in "Chemical Physics of Ionic Solutions," B. E. Conway and R. G. Barradas, Ed., John Wiley & Sons, Inc., New York, N. Y., 1966, p 295.

(6) See, *e.g.*, C. Tanford, *J. Phys. Chem.*, 59, 788 (1955).

(7) S. A. Rice and M. Nagasawa, "Polyelectrolyte Solutions," Academic Press, New York, N. Y., 1961, pp 99–118.

the Poisson–Boltzmann equation without making the Debye–Hückel approximation. The treatment, which is most similar to ours, is that of Gross and Strauss[8] which pertains to infinitely dilute polymer solutions of permeable and impermeable cylindrical polyelectrolytes. In the treatment of Gross and Strauss, it is assumed that there is no interaction between polymer molecules, and that each macromolecule is surrounded by an infinite amount of salt solution. Their approach is equivalent to that used by Wall and Berkowitz[9] for a spherical macromolecule. Instead of using the computational procedure of Wall and Berkowitz for the spherical macromolecule, Lifson[10] substituted a perturbation method which provided an analytical solution for the potential. Lifson's approach can also provide an analytical solution for the cylindrical model treated by Gross and Strauss. However, since we are interested in *finite* polymer concentrations in the present paper, the simplifications underlying the infinitely dilute solution treatment cannot be made (because the concentrations of counterions and co-ions are not equal at the symmetry surface between macromolecules, as they are at infinite dilution of polymer). Therefore, we have had to have recourse to a more detailed numerical computational procedure rather than use the analytical treatment of Lifson.

A model for the solution of multichain molecules at finite concentration is the cell model of the statistical theory of solutions. It is assumed that we may allocate to each of the $n_p$ macromolecules suspended in a volume $v$ (or $m_p$ moles per cm$^3$) a "cell" of volume $V = v/n_p = 1/Nm_p$, where $N$ is Avogadro's number. The shape of the cell is isomorphous with that of the macromolecule itself, and has the same height $h$ (see Figure 1). The radius $R$ of the cell is given by the condition $\pi R^2 h = V$. The volume of the multichain molecule is $\pi a^2 h$; hence, the volume fraction, $v_p$, of polymer in solution is given by

$$v_p = \frac{\pi a^2 h}{\pi R^2 h} = \frac{a^2}{R^2} \tag{1}$$

Since $R^2 = 1/\pi h m_p N$, $v_p = \pi a^2 h m_p N$. It will be observed that the model implies that the cylindrical molecules are arranged in a roughly parallel array so that, neglecting end effects, the electrostatic potential $\psi$ becomes a function of the radial coordinate $r$ only. The justification for the use of a parallel-array model derives from the important fact that there is a rather sharp drop in the potential from the polymer surface toward the boundary of the cell. In the region of $r = R$, the potential is fairly constant;[5] therefore, any deviation of the orientation of the macromolecules from the parallel arrangement will have little influence on the local value of $\psi$. Moreover, the electrostatic repulsion between the charged macromolecules will diminish the probability of density and orientational fluctuations; hence, the cell model is a reasonable one for charged macromolecules.

One should not be misled, because of the small variation in $\psi$ near $r = R$, into thinking that the cell-model treatment is equivalent to that for a single molecule in an infinite volume. The values of both $\psi$ and the ionic distribution depend on $R$, and should be evaluated explicitly.

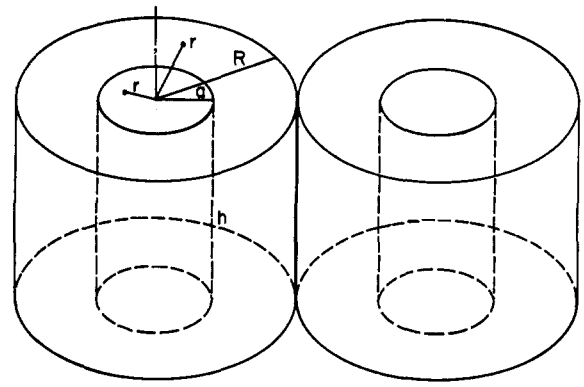


Figure 1. Cell model for the solution of multichain polymers. The cylindrical shape of the cell is isomorphous with that of the macromolecule, and has the same height $h$. The radii of the macromolecule and of the cell are $a$ and $R$, respectively. $r$ is a radial coordinate.

At the cell boundary the value of the potential is an extremum so that $(\partial\psi/\partial r)_R = 0$. For convenience, we take the value of $\psi$ at $R$ as our reference point of potential, *i.e.*, $\psi_R = 0$.

### Charge Distribution and Potential

The total number of ionizable groups (*i.e.*, carboxyl groups) per molecule is $Z$. At a given degree of ionization, $\alpha$, there will be $\nu$ charged sites per molecule, where $\alpha = \nu/Z$. Had the carboxylate ion groups been free negative charges, such as the electrons in a conductor, we would expect all the $\nu$ charges to accumulate at the surface of the cylinder. However, since the location of the carboxyl groups is fixed by the geometry of the macromolecule, such an accumulation is impossible. Moreover, the entropic losses accompanying the formation of any specified ionic conformation make the random homogeneous distribution of the charged groups sufficiently favorable as to enable us to make the assumption that the intramolecular charge density of the *fixed* ions is approximately constant and given by the over-all degree of ionization. Considering $\epsilon$ to be the numerical value of the electronic charge, we thus take the density, $\rho_f$, of the fixed charges as

$$\rho_f = \frac{-\nu\epsilon}{\pi a^2 h} \tag{2}$$

The solution contains $\nu$ positive monovalent counterions, as well as the negative polyion. While other workers[8,11] have assumed that association takes place between the counterions and the carboxylate ion groups, we have not made this assumption. For the sake of generality, we allow the solution to contain an excess of a uni-univalent salt (at a concentration of $n_s$ molecules per cm$^3$ or $m_s$ moles per cm$^3$) whose cation is the same as the counterions of the polyion. Even though it is possible to generalize this treatment to salts with multivalent counter- and/or co-ions, we restrict our calculations to uni-univalent salts since these are the ones of greatest interest. The rigorous calculation of the distribution of the counterions is a prohibitive task because of, among other things, excluded volume effects and

(8) L. M. Gross and U. P. Strauss in "Chemical Physics of Ionic Solutions," B. E. Conway and R. G. Barradas, Ed., John Wiley & Sons, Inc., New York, N. Y., 1966, p 361.
(9) F. T. Wall and J. Berkowitz, *J. Chem. Phys.*, **26**, 114 (1957).
(10) S. Lifson, *ibid.*, **27**, 700 (1957).
(11) F. T. Wall and R. H. Doremus, *J. Amer. Chem. Soc.*, **76**, 868 (1954).

possible ion-pair formation. Therefore, for lack of a better approximation, it is assumed[12] that the central field of the polyion induces a Boltzmann distribution of the small ions, both within and outside the cylindrical polyion. Thus, the charge density at any point in the solution will depend on $\alpha$, on the salt concentration, and on the polymer concentration. In order to evaluate the colligative properties of the system, it is necessary to compute $\psi$ at every point in the solution.

The molarity of the glutamic acid residues is $1000 \cdot m_p Z$. Since the polyion carries $\nu$ fixed negative charges, and since there are $\nu$ positive counterions associated with it, the concentrations (in moles/cm$^3$) of counterions, $m_+$, and co-ions, $m_-$, in the system are

$$m_+ = \nu m_p + m_s \tag{3}$$

and

$$m_- = m_s \tag{4}$$

Since we have assumed that the small ions obey a Boltzmann distribution, their *local* concentrations are given by

$$n_+ = n_+^0 e^{-\epsilon\psi/kT} \tag{5}$$

and

$$n_- = n_-^0 e^{\epsilon\psi/kT} \tag{6}$$

where $n_+^0$ and $n_-^0$ are the concentrations at $r = R$, where $\psi_R = 0$, and are given by the conservation conditions

$$\nu + n_s V = \int_0^R n_+ dV = 2\pi h n_+^0 \int_0^R e^{-\epsilon\psi/kT} r dr \tag{7}$$

and

$$n_s V = \int_0^R n_- dV = 2\pi h n_-^0 \int_0^R e^{\epsilon\psi/kT} r dr \tag{8}$$

or

$$n_+^0 = \left(\nu + n_s V\right) \Big/ 2\pi h \int_0^R e^{-\epsilon\psi/kT} r dr \tag{9}$$

and

$$n_-^0 = n_s V \Big/ 2\pi h \int_0^R e^{\epsilon\psi/kT} r dr \tag{10}$$

Since the macromolecule is permeable to the solvent and to the small mobile ions, we may assume that the potential, $\psi$, is the same on both sides of the surface of the polyion, *i.e.*, that the potential is continuous at this boundary (because a discontinuity in $\psi$ would imply an infinite local field), and that the electric field, $\partial\psi/\partial r$, is continuous across the boundary at $r = a$ (because no layer of free charges is assumed). Hence

$$\psi_{in}(a) = \psi_{ou}(a) \tag{11}$$

and

$$(\partial\psi_{in}/\partial r)_a = (\partial\psi_{ou}/\partial r)_a \tag{12}$$

where the subscripts in and ou refer to the inside and outside, respectively, of the polyion.

Because of the large (negative) value of $\psi$ inside the polyion, and also *near* the outside surface of the polyion, $e^{\epsilon\psi/kT}$ will be vanishingly small in these regions; hence, the negative co-ions are effectively expelled from these regions.

(12) Other assumptions about the distribution of the potential inside the macromolecule, which we have tried to use, did not give mathematical consistency.

### The Poisson–Boltzmann Equation

The electrostatic potential $\psi$ may be computed separately for the two regions $0 \leqq r \leqq a$ and $a \leqq r \leqq R$, and joined at $r = a$ by appropriate boundary conditions. Thus, the charge density, $\rho$, is evaluated separately for each region, and substituted in the Poisson equation. For this case of cylindrical symmetry, we obtain

$$\frac{1}{x}\frac{d}{dx}\left(x\frac{d\phi_{in}}{dx}\right) = (\kappa R)^2[1 + \lambda_- e^{\phi_{in}} - \lambda_+ e^{-\phi_{in}}] \tag{13}$$

$$\text{for } 0 \leq x \leq x_1$$

for the potential inside the polyion, and

$$\frac{1}{x}\frac{d}{dx}\left(x\frac{d\phi_{ou}}{dx}\right) = (\kappa R)^2[\lambda_- e^{\phi_{ou}} - \lambda_+ e^{\phi_{ou}}] \tag{14}$$

$$\text{for } x_1 \leq x \leq 1$$

for the potential outside the polyion, where $\rho$ is obtained from eq 2, 5, and 6

$$\phi = \epsilon\psi/kT \tag{15}$$

$$x = r/R \tag{16}$$

$$x_1 = a/R \tag{17}$$

$$\kappa^2 = \frac{4\nu\epsilon^2}{DkTa^2h} \tag{18}$$

where $D$ is the dielectric constant (assumed to be the same in the inner and outer regions), and

$$-\lambda_+ = \frac{n_+^0\epsilon}{\rho_f} = \frac{-\pi a^2 h n_+^0}{\nu} \tag{19}$$

$$-\lambda_- = \frac{n_-^0\epsilon}{\rho_f} = \frac{-\pi a^2 h n_-^0}{\nu} \tag{20}$$

It should be noted that the quantity of eq 18 is not the usual Debye–Hückel parameter $\kappa$, even though it has the same dimensions.

**Boundary Conditions.** The aforementioned boundary conditions may be written in terms of $x$ as

$$\phi_{x=1} = 0 \tag{21}$$

$$\left(\frac{d\phi}{dx}\right)_{x=1} = 0 \tag{22}$$

$$\phi_{in}(x_1) = \phi_{ou}(x_1) \tag{23}$$

$$(\partial\phi_{in}/\partial x)_{x_1} = (\partial\phi_{ou}/\partial x)_{x_1} \tag{24}$$

Also, eq 7 and 8 may be rewritten as

$$2\lambda_+ \int_0^1 e^{-\phi} x dx = L + v_p \tag{25}$$

and

$$2\lambda_- \int_0^1 e^{\phi} x dx = L \tag{26}$$

where

$$L = \frac{n_s \pi a^2 h}{\nu} \tag{27}$$

With these boundary conditions, it is possible to eval-

uate $\phi$ as a function of $x$ throughout the range $0 \leqq x \leqq 1$, or $\psi$ as a function of $r$ throughout the range $0 \leqq r \leqq R$, as indicated in a later section.

**Derived Quantities.** A knowledge of $\psi(r)$ leads immediately to the distribution of the mobile ions, $n_+(r)$ and $n_-(r)$, from eq 5 and 6, and to various electrochemical quantities, in particular those that can be measured in potentiometric titration and osmotic pressure experiments.

The potentiometric titration curve of a weak polyion containing a large number of the same kind of groups, with negligible nearest neighbor interactions, is given by the equation[13,14]

$$\mathrm{pH} = \mathrm{p}K_0 - \log \frac{1-\alpha}{\alpha} - 0.4343\frac{\epsilon\psi}{kT} \quad (28)$$

where $\mathrm{p}K_0$ is the intrinsic dissociation constant, $\alpha$ is the degree of dissociation at the given pH, and $\psi$ is the electrostatic potential on the surface of the polyion,[15] *i.e.*, at $r = a$. The term $-0.4343(\epsilon\psi/kT)$ is also designated $\Delta\mathrm{p}K$ to indicate that it is the contribution of the electrostatic field of the polyion to the standard free energy of ionization of a single group. We may write $\Delta\mathrm{p}K$ as

$$\Delta\mathrm{p}K = -0.4343\frac{\int_0^a \phi \mathrm{d}V}{\pi a^2 h} = \frac{-0.8686}{v_\mathrm{p}}\int_0^{x_1}\phi x\mathrm{d}x \quad (29)$$

The osmotic coefficient, $\varphi_\mathrm{p}$, is given by a generalization[5,16] of Langmuir's treatment[17,18] as the ratio of the real to the ideal osmotic pressures, $\pi_\mathrm{real}$ and $\pi_\mathrm{ideal}$. Now

$$\pi_\mathrm{real} = (n_+^0 + n_-^0)kT = \frac{-\rho_\mathrm{f}}{\epsilon}(\lambda_+ + \lambda_-)kT = \frac{\nu}{\pi a^2 h}(\lambda_+ + \lambda_-)kT \quad (30)$$

and

$$\pi_\mathrm{ideal} = (2n_\mathrm{s} + \nu/\pi R^2 h)kT \quad (31)$$

Hence

$$\varphi_\mathrm{p} = \frac{\nu}{\pi a^2 h}\frac{(\lambda_+ + \lambda_-)}{(2n_\mathrm{s} + \nu/\pi R^2 h)} = \frac{\lambda_+ + \lambda_-}{2L + v_\mathrm{p}} \quad (32)$$

It is seen from eq 30 that the parameters $\lambda_+$ and $\lambda_-$ determine the osmotic pressure.

It is also of interest to compute the fractions, $f_+$ and $f_-$, of the positive and negative ions inside the macromolecular cylinder. These are

$$f_+ = \frac{\int_0^a n_+^0 e^{-\epsilon\psi/kT}\mathrm{d}V}{n_\mathrm{s}\pi R^2 h + \nu} = \frac{\int_0^{x_1} e^{-\phi}x\mathrm{d}x}{\int_0^1 e^{-\phi}x\mathrm{d}x} \quad (33)$$

and

$$f_- = \frac{\int_0^{x_1} e^{\phi}x\mathrm{d}x}{\int_0^1 e^{\phi}x\mathrm{d}x} \quad (34)$$

**Parameters Used in Computation.** In all the calculations, the temperature was taken as 300°K. The values of $v_\mathrm{p}$ are based on dimensions of a polymer investigated by Goldstein,[2] assuming that the chains are either in the $\alpha$-helical or fully stretched conformations, respectively; the pertinent parameters are given in Table I.

**Table I.** Illustrative Parameters of Multichain Polyglutamic Acid[a] Required for Computation of $v_\mathrm{p}$

| Conformation | $h^b \times 10^8$ cm | $a^b \times 10^7$ cm | $v_\mathrm{p}$ | $R^c \times 10^6$ cm | $a/R$ |
|---|---|---|---|---|---|
| $\alpha$-Helical | 1.05 | 2.15 | 0.001096 | 6.50 | 0.0331 |
| Fully stretched | 2.52 | 5.02 | 0.0144 | 4.20 | 0.120 |

[a] This polymer had 70 lysine residues in the backbone (corresponding to 70 branches) and 12 glutamic acid residues per branch, or 840 carboxyl groups per molecule. The concentration of carboxyl groups in Goldstein's experiments[2] was $10^{-2}$ mole/l.; hence $m_\mathrm{p} = 1.19 \times 10^{-8}$ mole/ml. [b] In order to compute $h$ and $a$, the length per amino acid residue was taken as 1.5 and 3.6 Å for the $\alpha$-helical and fully stretched conformations, respectively. The length of the lysine side chain was taken as 3.5 and 7 Å in the $\alpha$-helical and fully stretched conformations, respectively. [c] Other values of $R$ were obtained for other concentrations, $m_\mathrm{p}$, using the relation $R^2 = 1/\pi h m_\mathrm{p} N$.

In order to present the data in compact form, the calculations were carried out for a discrete number of degrees of ionization, *viz.*, $\alpha = 0.2$, 0.4, 0.6, 0.8, and 1.0, corresponding to values of $\nu = 168$, 336, 504, 672, and 840, respectively. The salt concentration appears in the parameter $L$ of eq 27.

## Computational Procedure

Equations 13 and 14 were solved for $\phi(x)$ for various values of $\alpha$, salt concentration, and polymer concentration, using the Weizmann Institute CDC-1604 computer for numerical integration. An iteration method was used to obtain the quantities $\lambda_+$, $\lambda_-$, as well as $\phi(x)$. The details of the computations are available elsewhere.[19]

## Results and Discussion

For each value of $m_\mathrm{p}$, $n_\mathrm{s}$, and $\nu$ (and hence $L$), $\lambda_+$ and $\lambda_-$ were obtained by the iteration method described in the previous section. The values of $\lambda_+$ and $\lambda_-$ then yielded $n_+^0$ and $n_-^0$ from eq 19 and 20, respectively. Since $\phi(r)$ was also obtained from the solutions of eq 13 and 14, $n_+(r)$ and $n_-(r)$ were then computed from

(13) G. S. Hartley and J. W. Roe, *Trans. Faraday Soc.*, **36**, 101 (1940).
(14) A. Katchalsky, N. Shavit, and H. Eisenberg, *J. Polymer Sci.*, **13**, 69 (1954).
(15) Marcus[16] considers the potentiometric potential $\psi$ to be an average over the *fixed* polymeric charges. Since, in our case, the average density of the fixed charges is constant, the potential, adopting the view of Marcus, is equivalent to an average over the volume of the polymer. Hence, $\psi$ in eq 28 is a *measurable* quantity and no longer a function of $r$, but an average quantity given by eq 29.
(16) R. A. Marcus, *J. Chem. Phys.*, **23**, 1057 (1955).
(17) I. Langmuir, *ibid.*, **6**, 893 (1938).
(18) E. J. W. Verwey and J. T. Overbeek, "Theory of the Stability of Lyophobic Colloids," Elsevier Publishing Co., Amsterdam, 1948, p 90.
(19) These details have been deposited as Document No. NAPS-00573 with the ASIS National Auxiliary Publication Service, c/o CCM Information Corp., 909 3rd Ave., New York, N. Y. 10022. A copy may be secured by citing the document number and by remitting $1.00 for microfiche or $3.00 for photocopies. Advance payment is required. Make checks or money orders payable to: ASIS-NAPS.

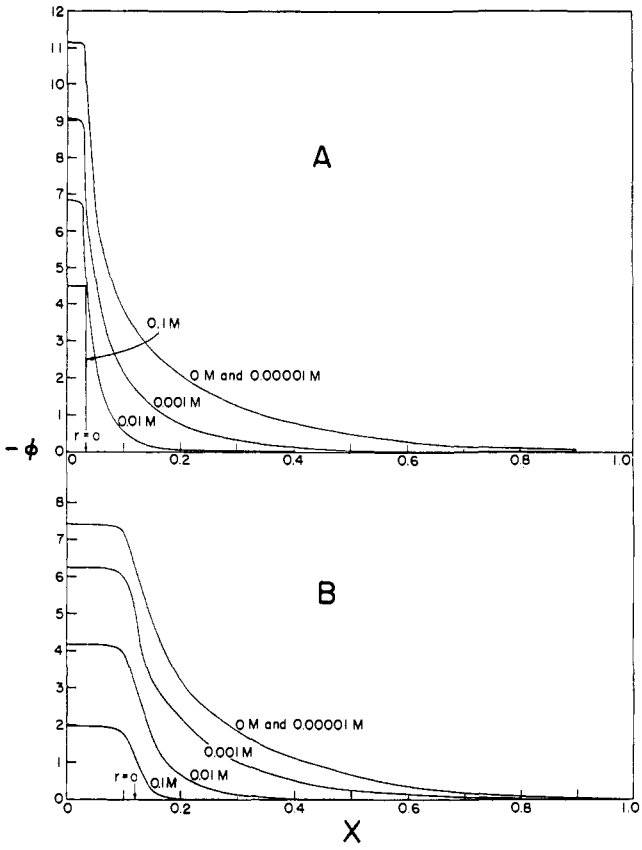


Figure 2. Values of $\phi$ as a function of $x$ for $\alpha = 1$ for (A) $\alpha$-helical ($R = 6.50 \times 10^{-6}$) and (B) stretched ($R = 4.20 \times 10^{-6}$) conformations at various salt concentrations at $T = 300°K$. The value of $x$, where $r = a$, is indicated by the arrow. The solution in (A) for 0.1 $M$ salt is the asymptotic one.

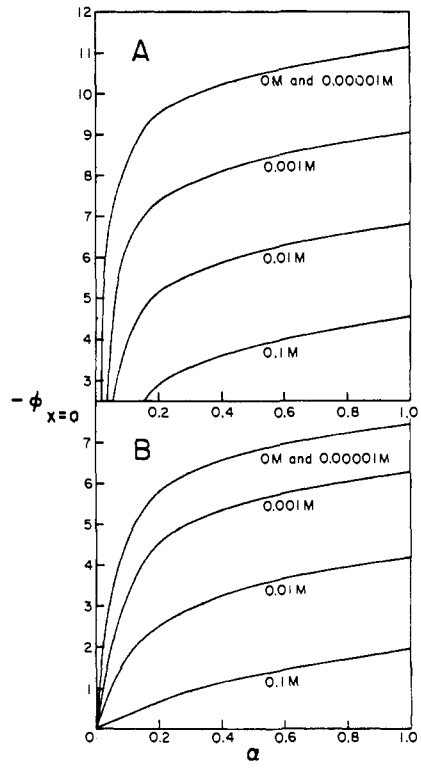


Figure 3. Dependence of $\phi_{x=0}$ on $\alpha$ at various salt concentrations for (A) $\alpha$-helical and (B) stretched conformations, for the values of $R$ shown in Figure 2.

eq 5 and 6, respectively; similarly $f_+$ and $f_-$ were computed from eq 33 and 34. Finally, $\Delta pK$ was obtained from eq 29 and $\varphi_p$ from eq 32.

For very large values of $n_s$ (in practice, for $n_s > 10^{19}$ molecules per cm$^3$), the computational procedure[19] becomes inaccurate. However, for high salt concentration, an asymptotic solution was obtained which is valid for $n_s \geq 10^{19}$ molecules per cm$^3$. The validity of this asymptotic solution is demonstrated elsewhere,[19] by comparing the parameters obtained with the exact and asymptotic theories, respectively, for $n_s = 6.03 \times 10^{18}$ (0.01 $M$).

Figure 2 is a plot of $\phi$ *vs.* $x$ for the helical and stretched conformations, respectively, for the data of Table I. It can be seen that the absolute values of $\phi$ are much larger than unity, especially at low salt concentration, from $x = 0$ up to several times the radius of the cylinder. Thus, the use of the Debye–Hückel approximation would have been invalid in this region of interest. It can also be seen that the absolute values of $\phi$ at $x = 0$ decrease markedly with increasing salt concentration. Figure 3 shows how $\phi$ at $x = 0$ increases with increasing $\alpha$. From Figures 2 and 3, it can be seen how $\phi$ is depressed with increasing salt concentration.

The potential determines the distribution of positive counterions and negative co-ions between the macromolecule and the surrounding medium. According to eq 5 and 6, the variations of $n_+(r)$ and $n_-(r)$, respectively, with $r$ follow the behavior of $\phi(r)$; *i.e.*, most of the counterions are drawn inside the molecule while the co-ions are expelled. A measure of this distribution of ions is given by $f_+$ and $f_-$, shown in Figures 4 and 5, respectively. It can be seen how these quantities vary with salt concentration and $\alpha$, and approach the limiting value of $(a/R)^2$ as $\alpha$ (and hence $\phi$) approaches zero (see eq 33 and 34). The potential also determines the variations of $\varphi_p$ and $\Delta pK$ with $\alpha$ at various salt concentrations (shown in Figures 6 and 7, respectively).

Table II shows the dependence of $\Delta pK$ on $\alpha$ and salt concentration. Table III shows the dependence of $\Delta pK$ on polymer concentration at three salt concentrations. This range of $m_p$ covers that of Goldstein's data.

**Table II.** Values of $\Delta pK$ for the Multichain Polymer[a] at Various Salt Concentrations at 30°

| Conformation | $\alpha$ | $\Delta pK$ 0[b] | 0.00001[b] | 0.001[b] | 0.01[b] | 0.1[b] | 1.0[b] |
|---|---|---|---|---|---|---|---|
| Helical | 0.2 | 3.99 | 3.96 | 3.05 | 2.09 | 1.26[c] | 0.36[c] |
| | 0.4 | 4.34 | 4.31 | 3.41 | 2.44 | 1.56[c] | 0.59[c] |
| | 0.6 | 4.54 | 4.51 | 3.61 | 2.64 | 1.74[c] | 0.75[c] |
| | 0.8 | 4.67 | 4.65 | 3.75 | 2.78 | 1.86[c] | 0.87[c] |
| | 1.0 | 4.78 | 4.75 | 3.85 | 2.88 | 1.96[c] | 0.97[c] |
| Stretched | 0.2 | 2.29 | 2.28 | 1.77 | 0.92 | 0.23 | 0.030[c] |
| | 0.4 | 2.67 | 2.66 | 2.15 | 1.27 | 0.42 | 0.060[c] |
| | 0.6 | 2.87 | 2.86 | 2.35 | 1.47 | 0.57 | 0.090[c] |
| | 0.8 | 3.01 | 3.00 | 2.49 | 1.61 | 0.66 | 0.12[c] |
| | 1.0 | 3.12 | 3.11 | 2.57 | 1.72 | 0.78 | 0.15[c] |

[a] At a polymer concentration of $m_p = 1.19 \times 10^{-8}$ mole/ml. [b] Salt concentration in moles/l. [c] Values from asymptotic solution.

**Calculation of Donnan Ratio.** A multichain polyelectrolyte can be involved in two types of Donnan equilibria, one between the macromolecule and its

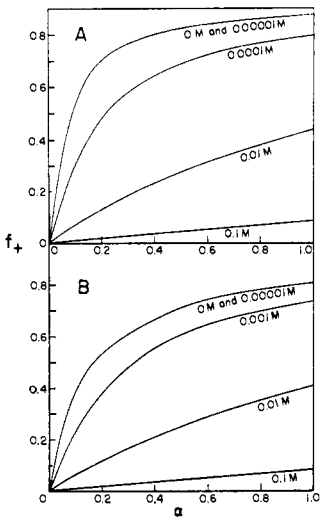


Figure 4. Variation of $f_+$ with $\alpha$ for (A) $\alpha$-helical ($R = 6.50 \times 10^{-6}$) and (B) stretched ($R = 4.20 \times 10^{-6}$) conformations at various salt concentrations at $T = 300°K$. The values of $f_+$ at 1.0 $M$ salt are too small to show on this scale.

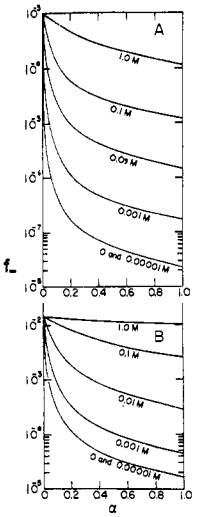


Figure 5. Variation of $f_-$ with $\alpha$ for (A) $\alpha$-helical ($R = 6.50 \times 10^{-6}$) and (B) stretched ($R = 4.20 \times 10^{-6}$) conformations at various salt concentrations at $T = 300°K$.

surroundings, and the other an equilibrium across a membrane which separates the polymer solution from a polymer-free one. In this section, we consider the former type and compare the values of $\Delta pK$, computed from eq 28 and 29, with those obtained by assuming the existence of a Donnan equilibrium between the macromolecule and its surroundings. In the next section, we will consider the Donnan equilibrium across a membrane.

To compute $\Delta pK$, we write $f_+$ (defined in eq 33) as

$$f_+ = \frac{(n_+)_{in}\pi a^2 h}{(n_+)_{in}\pi a^2 h + (n_+)_{ou}\pi(R^2 - a^2)h} \quad (35)$$

Hence, the Donnan ratio becomes

$$\frac{(n_+)_{in}}{(n_+)_{ou}} = \left(\frac{R^2 - a^2}{a^2}\right)\left(\frac{f_+}{1 - f_+}\right) \quad (36)$$

The Donnan potential for the macromolecule, regarded

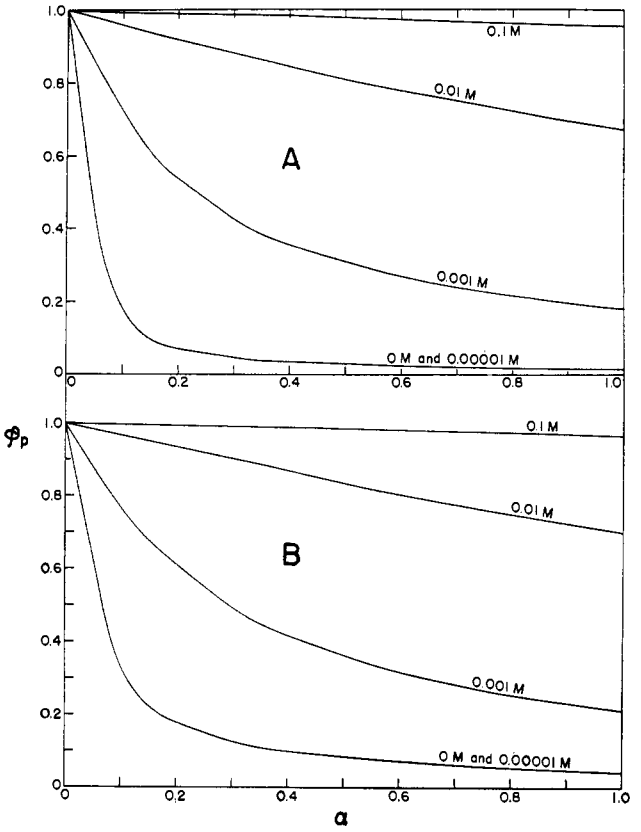


Figure 6. Values of $\varphi_p$ as a function of $\alpha$ for (A) $\alpha$-helical ($R = 6.50 \times 10^{-6}$) and (B) stretched ($R = 4.20 \times 10^{-6}$) conformations at various salt concentrations at $T = 300°K$.

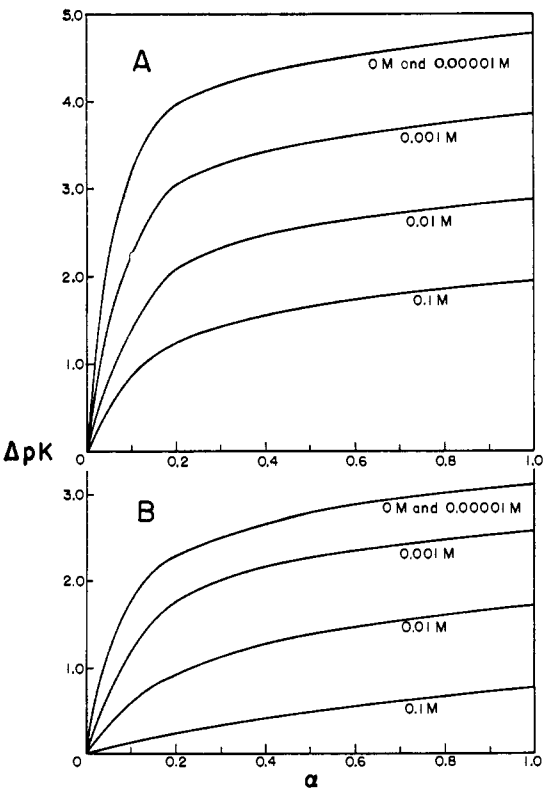


Figure 7. Variation of $\Delta pK$ with $\alpha$ for (A) $\alpha$-helical ($R = 6.50 \times 10^{-6}$) and (B) stretched ($R = 4.20 \times 10^{-6}$) conformations at various salt concentrations at $T = 300°K$.

Table III. Dependence of $\Delta pK$ on Polymer Concentration

| Conformation | Salt concn, $M$ | Concn of carboxyl groups, mole/l. | $m_p$, mole/ml | $R \times 10^6$, cm | $\Delta pK$ $\alpha = 0.2$ | $\alpha = 0.4$ | $\alpha = 0.6$ | $\alpha = 0.8$ | $\alpha = 1.0$ |
|---|---|---|---|---|---|---|---|---|---|
| Helical | 0.001 | 0.0020 | $2.38 \times 10^{-9}$ | 14.5 | 3.07 | 3.44 | 3.64 | 3.78 | 3.88 |
| | | 0.010 | $1.19 \times 10^{-8}$ | 6.50 | 3.05 | 3.41 | 3.61 | 3.75 | 3.85 |
| | | 0.100 | $1.19 \times 10^{-7}$ | 2.06 | 2.71 | 3.06 | 3.25 | 3.39 | 3.66 |
| | 0.01 | 0.0020 | $2.38 \times 10^{-9}$ | 14.5 | 2.26[a] | 2.56[a] | 2.74[a] | 2.86[a] | 2.96[a] |
| | | 0.010 | $1.19 \times 10^{-8}$ | 6.50 | 2.09 | 2.44 | 2.64 | 2.78 | 2.88 |
| | | 0.100 | $1.19 \times 10^{-7}$ | 2.06 | 2.05 | 2.40 | 2.59 | 2.73 | 2.83 |
| | 0.1 | 0.0020 | $2.38 \times 10^{-9}$ | 14.5 | 1.26[a] | 1.56[a] | 1.74[a] | 1.86[a] | 1.96[a] |
| | | 0.010 | $1.19 \times 10^{-8}$ | 6.50 | 1.26[a] | 1.56[a] | 1.74[a] | 1.86[a] | 1.96[a] |
| | | 0.100 | $1.19 \times 10^{-7}$ | 2.06 | 1.12[b] | 1.45[b] | 1.64[b] | 1.78[b] | 1.88[b] |
| | 1.0 | 0.0020 | $2.38 \times 10^{-9}$ | 14.5 | 0.36[a] | 0.59[a] | 0.75[a] | 0.87[a] | 0.97[a] |
| | | 0.010 | $1.19 \times 10^{-8}$ | 6.50 | 0.36[a] | 0.59[a] | 0.75[a] | 0.87[a] | 0.97[a] |
| | | 0.100 | $1.19 \times 10^{-7}$ | 2.06 | 0.35[a] | 0.59[a] | 0.75[a] | 0.87[a] | 0.96[a] |
| Stretched | 0.001 | 0.0020 | $2.38 \times 10^{-9}$ | 9.39 | 1.85 | 2.24 | 2.46 | 2.60 | 2.72 |
| | | 0.010 | $1.19 \times 10^{-8}$ | 4.20 | 1.77 | 2.15 | 2.35 | 2.49 | 2.57 |
| | | 0.100 | $1.19 \times 10^{-7}$ | 1.33 | 1.09 | 1.39 | 1.56 | 1.69 | 1.78 |
| | 0.01 | 0.0020 | $2.38 \times 10^{-9}$ | 9.39 | 0.94 | 1.28 | 1.48 | 1.62 | 1.73 |
| | | 0.010 | $1.19 \times 10^{-8}$ | 4.20 | 0.92 | 1.27 | 1.47 | 1.61 | 1.72 |
| | | 0.100 | $1.19 \times 10^{-7}$ | 1.33 | 0.78 | 1.08 | 1.25 | 1.38 | 1.48 |
| | 0.1 | 0.0020 | $2.38 \times 10^{-9}$ | 9.39 | 0.28[a] | 0.49[a] | 0.64[a] | 0.76[a] | 0.85[a] |
| | | 0.010 | $1.19 \times 10^{-8}$ | 4.20 | 0.23[c] | 0.42[c] | 0.57[c] | 0.66[c] | 0.78[c] |
| | | 0.100 | $1.19 \times 10^{-7}$ | 1.33 | 0.22 (0.27)[a] | 0.39 (0.46)[a] | 0.52 (0.60)[a] | 0.63 (0.71)[a] | 0.71 (0.80)[a] |
| | 1.0 | 0.0020 | $2.38 \times 10^{-9}$ | 9.39 | 0.030[a] | 0.060[a] | 0.090[a] | 0.12[a] | 0.15[a] |
| | | 0.010 | $1.19 \times 10^{-8}$ | 4.20 | 0.030[a] | 0.060[a] | 0.090[a] | 0.12[a] | 0.15[a] |
| | | 0.100 | $1.19 \times 10^{-7}$ | 1.33 | 0.030[a] | 0.059[a] | 0.088[a] | 0.12[a] | 0.14[a] |

[a] Values from asymptotic solution. [b] In the asymptotic solution, these values are the same as for $R = 6.50 \times 10^{-6}$. [c] In the asymptotic solution, these values are the same as for $R = 9.39 \times 10^{-6}$.

as a phase, may be defined as

$$\log \frac{(n_+)_{in}}{(n_+)_{ou}} = 0.4343\frac{\epsilon\psi}{kT} = -\Delta pK \qquad (37)$$

Since the potentiometric $\psi$ is independent[15] of $r$, the last equality of eq 37 is an identification of $\Delta pK$ with the macroscopic Donnan potential. Making use of eq 36, eq 37 becomes

$$-\Delta pK = \log\left(\frac{R^2 - a^2}{a^2}\right) + \log\left(\frac{f_+}{1 - f_+}\right) \qquad (38)$$

Equation 38 should hold at the higher salt concentrations, where the ion atmosphere is denser, and a clearer distinction can be made between the macromolecular and solution phases; this is verified by the data in Table IV, where it is seen that eq 38 holds for salt concentrations of approximately 0.01 $M$ and higher.

**Donnan Equilibrium across a Membrane.** Consider a polyelectrolyte solution at concentration $m_p$ to be in equilibrium across a membrane with a salt solution of concentration $n_s'$. The Boltzmann distribution implies that the electrochemical potentials of the positive and negative ions, respectively, in the polymer solution are independent of $r$, and hence can be set equal to their values at $r = R$. It then follows that

$$n_s'^2 = n_+^0 n_-^0 \qquad (39)$$

Since $n_+^0$ and $n_-^0$ have been computed for each value of $m_p$, $n_s$, and $\nu$ from eq 19 and 20, we immediately obtain $n_s'$ from eq 39.

The Donnan equilibrium across the membrane may be expressed in terms of the quantity $\Gamma$ defined as

$$\Gamma = \frac{n_s' - n_s}{Nm_p(\nu/\alpha)} \qquad (40)$$

Table IV. Comparison of $\Delta pK$ Values with Those Computed from Donnan Potential for the Helical Conformation at a Polymer Concentration of $m_p = 1.19 \times 10^{-8}$ mole/ml

| Salt concn, $M$ | $\alpha$ | $\Delta pK$ from Eq 28 and 29 | Eq 38 |
|---|---|---|---|
| 0.001 | 0.2 | 3.05 | 2.91 |
| | 0.4 | 3.41 | 3.21 |
| | 0.6 | 3.61 | 3.37 |
| | 0.8 | 3.75 | 3.48 |
| | 1.0 | 3.85 | 3.56 |
| 0.01 | 0.2 | 2.09 | 2.09 |
| | 0.4 | 2.44 | 2.44 |
| | 0.6 | 2.64 | 2.62 |
| | 0.8 | 2.78 | 2.75 |
| | 1.0 | 2.88 | 2.85 |
| 0.1 | 0.2 | 1.26 | 1.26 |
| | 0.4 | 1.56 | 1.56 |
| | 0.6 | 1.74 | 1.74 |
| | 0.8 | 1.86 | 1.86 |
| | 1.0 | 1.96 | 1.96 |

Table V. Dependence of $\Gamma$ on Polymer Concentration[a]

| Conformation | $m_p$, mole/cm$^3$ | $\Gamma$ |
|---|---|---|
| Helical | $1.19 \times 10^{-8}$ | 0.011 |
| | $1.19 \times 10^{-7}$ | 0.015 |
| Stretched | $1.19 \times 10^{-8}$ | 0.057 |
| | $1.19 \times 10^{-7}$ | 0.067 |

[a] For $n_s = 6.03 \times 10^{18}$ (0.01 $M$), $\alpha = 1.0$.

The treatment in this section emphasizes the difference between our treatment for *finite* polymer concentration, compared to that of Gross and Strauss[8] for a polymer at infinite dilution. Thus, we are able to compute the dependence of $\Gamma$ on $m_p$, as shown in Table V. Some experimental values of $\Gamma$ for linear polyelectrolytes at 0.01 $M$ salt[20] are of the same order of magnitude as those

(20) See Figure 9 of ref 5.

shown in Table V for the stretched conformation (which is more like the linear polymer than is the helical multichain polymer).

**Comparison between Computed and Experimental $\Delta pK$ values.** Some of the data of Table II are plotted in Figure 8 together with experimental data of Goldstein.[2] The departure of the experimental carboxyl group concentrations (cited in the legend) from 0.01 $M$ is neglected in the comparison with the experimental results, since these deviations have a negligible effect on $\Delta pK$, as can be seen from the data of Table III. The experimental values of $\Delta pK$ were computed as [pH $-$ log $\alpha/(1-\alpha)$ $-$ p$K_0$], according to eq 28.

A preliminary examination of the experimental data indicated that the value of p$K_0$ differed by several tenths of a p$K$ unit for the helical and for the stretched conformations, an observation also reported by Hermans[21] for the helical and randomly coiled forms of linear poly-L-glutamic acid, and detectable in the data of Nylund and Miller[22] for the same linear polymer.[23] This difference may be rationalized by realizing that eq 28 is incomplete in attributing $\Delta pK$ solely to electrostatic effects. Actually, $\Delta pK$ should be written as

$$\Delta pK = \Delta pK_{elec} + \Delta pK_{HB} + \Delta pK_{conf} \qquad (41)$$

where $\Delta pK_{elec}$ is the electrostatic contribution computed in this paper, $\Delta pK_{HB}$ is a contribution arising from possible hydrogen bonding[24] between un-ionized side-chain carboxyl groups, and $\Delta pK_{conf}$ is a contribution arising from nonspecifiable conformation effects which may influence the degree of accessibility of the carboxyl groups. As a result, the p$K_0$ of eq 28 is really

$$pK_0 = pK_0^{int} + \Delta pK_{HB} + \Delta pK_{conf} \qquad (42)$$

where p$K_0^{int}$ is the intrinsic p$K_0$ that would be observed for a model compound, in the absence of all the $\Delta pK$ contributions. While one can rationalize the difference in p$K_0$ between the helical and stretched conformations in terms of differences in $\Delta pK_{HB}$ and $\Delta pK_{conf}$, respectively (*e.g.*, by estimating the effect[24] of a different degree of hydrogen bonding in both conformations), we prefer to rely on the experimental observation, made here and in the literature,[21-23] that such differences exist. Accordingly, we may account for the data of Figure 8 by assigning p$K_0$ values of 4.60 and 4.30 to the stretched and helical conformations, respectively.

Since a preliminary examination of the data indicated that the conformation was probably essentially helical at all values of $\alpha$ at 1.0 $M$ salt (except perhaps at *very high* values of $\alpha$), and essentially stretched at all values of $\alpha$ at 0.01 $M$ salt (except perhaps at *very low* values of $\alpha$), the p$K_0$ values used to obtain the experimental data of Figure 8, at these salt concentrations, were 4.30 and 4.60, respectively. For the intermediate concentration, 0.1 $M$ salt, where we may expect a more pronounced

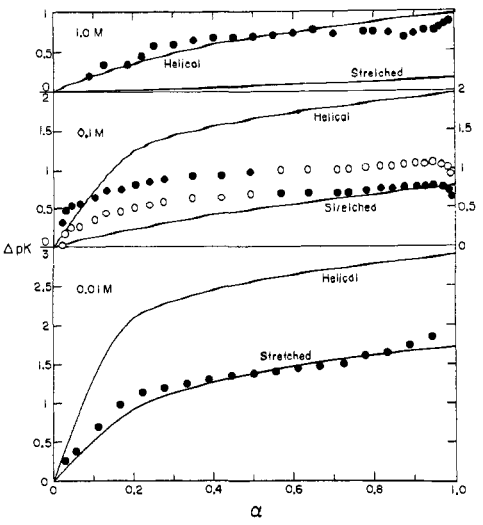


Figure 8. Dependence of $\Delta pK$ on $\alpha$ at 1.0, 0.1, and 0.01 $M$ salt at 30°; the concentration of carboxyl groups at each of these salt concentrations was 0.008, 0.014, and 0.0018, respectively. The curves are theoretical (from the data of Table II for helical and stretched conformations, respectively) and the points are experimental[2] [computed from the following values of p$K_0$, as discussed in the text: at 1.0 $M$, p$K_0$ = 4.30; at 0.1 $M$, p$K_0$ = 4.3 for $\alpha < 0.5$ and 4.6 for $\alpha > 0.5$ (solid circles) (the open circles are the experimental data for p$K_0$ = 4.6 for $\alpha < 0.5$ and 4.3 for $\alpha > 0.5$); at 0.01 $M$, p$K_0$ = 4.60].

helix → stretched transition as $\alpha$ is increased, we have used p$K_0$ = 4.30 for $0 < \alpha < 0.5$ and 4.60 for $0.5 < \alpha < 1.0$ (the *filled* circles in Figure 8); it is not intended to imply that p$K_0$ changes abruptly at $\alpha = 0.5$, but rather that there is a uniform change in p$K_0$ in this region of $\alpha$. It can be seen from Figure 8, that the use of these p$K_0$'s is consistent with the interpretation that the polymer is essentially in the helical and stretched conformations at high and low salt concentrations, respectively, at almost all values of $\alpha$, but that, at intermediate salt concentrations (~0.1 $M$), an increase of $\alpha$ leads to a change of conformation from the helix to the stretched state.

**Comparison between Computed and Experimental $\varphi_p$ Values.** An unpublished rough measurement of $\varphi_p$ in the absence of salt (made by Alexandrowicz) indicates that the order of magnitude of the experimental value (~0.15 for the sodium salt in water) is the same as that computed for the stretched conformation at moderately high values of $\alpha$ (see Figure 6).

**Comparison with "Infinite Dilution" Theories.** As already pointed out, the Wall–Berkowitz[9] and Lifson[10] solutions for spherical polyelectrolytes and the Gross–Strauss[8] solution for cylindrical ones apply to polymers at infinite dilution. In contrast to these treatments, in which the electrostatic potential falls to zero at infinite distance from the polymer (and, therefore, the theory applies only at infinite dilution of polymer), our results apply at finite polymer concentration, with the potential falling to zero at the boundary of the cell, *i.e.*, at $r = R$ (see Figure 1). From a comparison of our results with those of Wall–Berkowitz, Lifson, and Gross–Strauss, it is found that our results extrapolate to theirs at infinite dilution (where our $R$ approaches infinity).

(21) J. Hermans, Jr., *J. Phys. Chem.*, 70, 510 (1966).
(22) R. E. Nylund and W. G. Miller, *J. Amer. Chem. Soc.*, 87, 3537 (1965).
(23) See also A. Wada, *Mol. Phys.*, 3, 409 (1960), M. Nagasawa and A. Holtzer, *J. Amer. Chem. Soc.*, 86, 538 (1964), and H. J. Sage and G. D. Fasman, *Biochemistry*, 5, 286 (1966), for a similar effect.
(24) M. Laskowski, Jr., and H. A. Scheraga, *J. Amer. Chem. Soc.*, 76, 6305 (1954).